ORIGINAL ARTICLE

Characterization and digestogram modeling of modified elephant foot yam (*Amorphophallus paeoniifolius*) starch using ultrasonic pretreated autoclaving

Sreejani Barua[1,2] | Karan Tudu[1] | Madhulekha Rakshit[1] |
Prem Prakash Srivastav[1]

[1]Department of Agricultural and Food Engineering, Indian Institute of Technology Kharagpur, Kharagpur

[2]Max Planck Institute for Polymer Research, Mainz. Ackermannweg 10, Mainz

Correspondence
Sreejani Barua, Department of Agricultural and Food Engineering, Indian Institute of Technology Kharagpur, Kharagpur 721302, India.
Email: sreejani301@iitkgp.ac.in

Abstract

Native elephant foot yam starch (EFYS) is highly digestible, and it is not recommendable for consumption by diabetic and obese people. To address this problem, the current study focuses on the amendments in various properties (such as functional properties, whiteness index, amylose content, morphology, and digestion) of EFYS using ultrasonication (US) and US pretreated autoclave (AL) modification with varied time viz. 15, 30, and 45 min. Both the treatments enhanced the water absorption, swelling power, and solubility of EFYS. US-assisted AL treatment was responsible for increasing the resistant starch (RS) fraction and the highest increment was observed in US-AL45 EFYS (39.13 ± 1.19 %) as compared to the native counterpart (30.65 ± 1.06 %). Molecular aggregations were observed in all US-AL EFYS, whereas US treatment broke the agglomerations and increased the intergranular spaces. FTIR analysis revealed the highest increase in ordered to amorphous starch (1047/1022 cm^{-1}) in US-AL45 EFYS followed by native and others modified EFYS. The highest increase in amylose content was notable in US-AL45 (10.02 ± 0.08 %) as compared to other native and others treated EFYS. To understand the kinetic behavior of the native and modified EFYS, first-order kinetics, Michaelis–Menten, Paolucci Jeanjean, Logistic, and Weibull models were applied. The digestogram models highlighted the highest digestibility in native EFYS, preceded by US, US-AL 15, US-AL 30, and US-AL 45 EFYS. US-AL 45 EFYS showed the highest change in all the functional properties as compared to native and other modified EFYS.

Practical applications

Owing to the prevalent lifestyle diseases, a continuous evolution in nutritional behaviors has emerged. Although starch imparts consistency and quality to the commercial food products, its high digestibility results in harmful effects to diabetic and obese patients. Elephant foot yam is considered as a unique source of starch and its modification leads to a decrease in enzyme hydrolysis while making it health beneficial. Ultrasonic pretreated autoclaving is one such potential physical modification treatment which can facilitate toward decrease in enzyme digestibility of elephant foot yam starch (EFYS), yet enhancing

its swelling properties that in turn leads to the growth of functional food processing industry. The findings of the study highlight the enzyme digestogram modeling of US and US-AL modified EFYS in order to shed light on the mechanism that regulates them.

1 | INTRODUCTION

Elephant foot yam (*Amorphophallus paeoniifolius*) is a tropical tuber crop mainly cultivated in South East Asia countries, Africa, Pacific regions. This stem tube falls under Araceae family and is frequently used for preparing curry and pickle. It has achieved the status of a cash crop due to its high yield of production (50–80 t/ha), low production expenses, high market acceptability, and profitable economic returns (Singh & Sharanagat, 2020). It is a promising source of starch and also contains substantial quantity of minerals which includes potassium, iron, calcium, and phosphorous (Nagar, Sharanagat, Kumar, Singh, & Mani, 2019).

Digestion of starch is a very interesting phenomenon, consisting of three important phases. Relatively rapidly digestible starch (RDS) and slowly digestible starch (SDS) are the starch fractions that are digestible within 20 and 120 min after intake, respectively. The fraction of starch which is not digestible after 120 min of digestion is referred to as resistant starch (RS) and considered as an important functional polymeric carbohydrate ingredient for the digestion process (Barua, Khuntia, Srivastav, & Vilgis, 2021; Barua, Rakshit, & Srivastav, 2021; Barua & Srivastav, 2017). RS acts as a beneficial ingredient for lowering the starch digestibility which is helpful for diabetic and obese patients. In the food processing industry, starch is commonly used as a functional additive and a large section of the starch used worldwide is obtained from traditional sources such as potato, rice, wheat, and maize. Due to its higher digestibility and lower consistency under higher shear force, temperature, and also poor solubility in common organic solvents, various modification techniques, such as physical, chemical, and enzymatic treatments have been introduced (Li, Li, & Zhu, 2018). The disadvantages of using chemical and enzymatic treatments include the formation of chemical residues and the presence of high sensitivity of enzyme to temperature, pressure, pH, and salty ions, respectively (Hu et al., 2013). So, to alter the characteristics of starch, various physical modification techniques have been employed to enhance the functionalities of native starch.

Physical modification using ultrasonication (US) is considered as a green technology and has been applied in food industries for several years. US can produce liquid cavitation and mechanical action. Formation of cavitation leads to the development of active radicals such as $\bullet OH$, $\bullet O$, and $\bullet HO_2$. The newly created active radicals are responsible for attacking the starch granules and altering the properties (Hu et al., 2013). Various studies have been conducted on the modification of starch using autoclave (AL) treatment (Babu & Parimalavalli, 2013; Dundar & Gocmen, 2013; Jagannadham, Parimalavalli, & Babu, 2014). Based on the previous studies, it was depicted that the combination of US and AL have not been studied for modifying elephant foot yam starch (EFYS). Also different digestogram models have not been employed earlier to study the digestion kinetics of US and US-assisted

AL-treated EFYS. Therefore, the objectives of the study are established as follows: (a) to document the changes in the functional properties of US and US-AL modified EFYS; (b) to understand the morphology of native and modified (US and US-AL) EFYS; (c) to evaluate the digestogram kinetic parameters of the native, US, and US-AL modified EFYS using mathematical and empirical models.

2 | MATERIAL AND METHODS

2.1 | Materials

Elephant foot yam was acquired from Bidhan Chandra Krishi Vishwavidlaya, West Bengal, India. α-amylase from porcine pancreas (A3176-1MU, activity 16 U/mg solid) and amyloglucosidase from *Aspergillus niger* (A7 420-25MG, activity 30–60 U/mg) were purchased from Sigma Chemical Company (St. Louis, MO). GOD-POD, endpoint assay, and kinetic assay kit were procured from ARKRAY Healthcare Pvt. Ltd., Surat, India. The chemicals and solvents used were of scientific grade.

2.2 | Starch isolation

Isolation of starch was carried out using the method described by Sukhija, Singh, and Riar (2016a, 2016b). After the washing, peeling, and shredding of the tuber crops, it was dipped in the potassium metabisulphite (0.25 %) and citric acid (0.12 %) solution for 1 hr which served as preservative and antibacterial agents, respectively. The shreds were then ground for 2 min in a lab grinder with the addition of water. The filtered starch slurry was obtained using 300 mesh (BSS) sieve and the filtrate was allowed to settle down at 4°C for 90 min. Decantation of the supernatant followed by repeated washing were performed and finally 0.25% NaOH was added. The solution was allowed to settle down and the precipitation was washed 3–5 times repeatedly until the neutral pH was obtained. The starch slurry was centrifuged at 3,000 rpm for 10 min and the purified starch was collected from the bottom of the sediment. The obtained starch cake was transferred to trays and dried overnight in a cabinet drier at 40°C.

2.3 | Modification of starch

EFYS was modified using two different methods: (a) US modification, performed using an Ultrasonic Processor (UP50H, Dr. Hielscher 50W model, manufactured by Dr. Hielscher Gmbh, Teltow, Germany),

equipped with a standard sonotrode of 1 mm diameter probe, operating at 25 kHz for 30 min. Starch slurry of 30 % w/w was used for US modification and the modified starch was denoted as US EFYS. (b) Autoclave modification for US pretreated samples using laboratory autoclave (Model RA-PC, manufactured by Reico Equipment & Instrument Pvt. Ltd, Kolkata, India). The treatments were carried out at 120 °C for 15, 30, and 45 min and were denoted as US-AL15, US-AL30, US-AL45, respectively. The starch samples treated with both the methods were allowed for drying overnight at 40 °C using hot air oven (Heraeus oven, manufactured by Thermo Fisher Scientific, Waltham, MA) until the moisture content was 5–6 %.

2.4 | Functional properties

Water absorption capacity (WAC) was determined with slight modification by using the method defined by Wani, Hamid, Hamdani, Gani, and Ashwar (2017). Starch samples (3 g) were weighed in preweighted labeled centrifuge tubes and 25 mL of water was added in each centrifuge tube. The tubes containing the starch water mixture were shaken vigorously for 10 min and were kept at 25 °C for allowing the water absorption. After 30 min the starch water mixture was centrifuged at 3,000 rpm for 15 min. The excess water was drained away and the tubes were dried at 50 °C for 25 min in a hot air oven. The final weight of the sample and the tube was calculated and WAC (g/g) was determined using the following Equation (1):

$$WAC \left(\frac{g}{g}\right) =$$

$$\frac{\text{Weight of sample with tube after drying} - \text{weight of tube} - \text{weight of sample}}{\text{Weight of sample}}.$$

$$(1)$$

Swelling power (SP) and solubility (SL) were determined by the method described by Nattapulwat, Purkkao, and Suwithayapan (2009) with slight modifications. The mixture of sample (1 g, dry basis) and 25 mL distilled water was allowed to heat at 90 °C with continuous shaking for 30 min. After the shaking, centrifugation of the samples was performed at 4,000 rpm for 15 min and the residue obtained after drying the supernatant at 105 °C for 3.5 h was considered as the dissolved starch and used for the calculation of solubility. The SP and SL were determined using the following Equations (2) and (3):

$$\text{Swelling power} \left(\frac{g}{g}\right) = \frac{\text{Weight of sediment}}{\text{Weight of dry starch} - \text{weight of dissolved starch}},$$

$$(2)$$

$$\text{Solubility} (\%) = \frac{\text{Dried solid weight of supernatant}}{\text{Weight of dry sample}}.$$

$$(3)$$

2.5 | Whiteness index (WI)

WI of the starch was measured using a portable colorimeter (Konica Minolta Sensing, Inc., Osaka, Japan) using L^* (lightness), a^* (red-green),

and b^* (yellow-blue) color spaces at continuous lighting environments. The following Equation (4) is used to measure the whiteness index:

$$WI = \sqrt{100 - (100 - L*)^2 + (a*)^2 + (b*)^2}. \quad (4)$$

2.6 | Amylose content

The amylose content was determined by colorimetric method described by McGrance, Cornell, and Rix (1998). Pure potato amylose type III (HiMedia, Mumbai, India) was used for preparing the standard curve.

2.7 | SEM image capturing

Granular structures of both native and modified starches were observed under scanning electron microscope (SEM) (Zeiss EVO 60, Carl Zeiss SMT, Wetzlar, Germany). Starch samples were prepared by sprinkling the starch on double-sided adhesive tape attached to a circular aluminum stub and then coated with 20 nm gold under vacuum. The samples were viewed and photographed in a scanning electron microscope (Bruker D2 phase second generation, Billerica, Massachusetts, USA) at an accelerating potential of 20 kV.

2.8 | Functional group analysis

Different groups present in native and modified starches were identified by FTIR analysis. All spectra were collected through Nicolet 6700 FTIR manufactured by Thermo Fisher Scientific. The starch nanoparticles were mixed with KBr at a ratio of 1:100 and pressed into tablets before measurements. A region of 500–4,000 cm^{-1} was used with a resolution of 4 cm^{-1} and 32 scans.

2.9 | Measurement of starch digestion fractions

RDS, SDS, and RS fractions of native and modified EFYS were estimated according to the method described by Ye, Lu, Yao, Gan, and Sui (2016). Screw cap glass tubes containing 50 mg of sample and 10 mL of water were subjected to continuous heating with frequent mixing. Sodium acetate buffer (0.5 M) of pH 5.2 was added (10 mL) to the cold solution after 20 min of heating. The vortex mixer (Ika Vortex Genius 3) was used for vigorous mixing of the solution. Enzyme solution of 1 mL containing amyloglucosidase (35 U/mg) and pancreatic α-amylase (50 U/mg) was added to the solution and permitted to incubate into a shaking water bath (RWBS, Reico Equipment & Instrument Pvt. Ltd., India) (220 strokes/min) at 37 °C for 20 and 120 min. Released glucose of 2 mL aliquots at 20 and 120 min were measured using GOD-POD kit and a spectrometer (Varian 50 Bio UV–visible spectrometer) at 510 nm. Glucose to starch conversion factor 0.9 was used. Equations (5)–(7) depicts the fraction of RDS, SDS, and RS content, respectively,

$$RDS\,(\%) = SDS_{20}\,(\%), \tag{5}$$

$$SDS\,(\%) = SDS_{120}\,(\%) - SDS_{20}\,(\%), \tag{6}$$

$$RS\,(\%) = 99.09\,(\%) - SDS_{120}\,(\%). \tag{7}$$

SDS_{20} (%) represents the amount of RDS content at 20 min and SDS_{120} corresponds to the amount of SDS content at 120 min in the starch. The purity of extracted EFYS was 99.09 %.

2.10 | Measurement of starch digestogram

The degree of hydrolyzed starch was calculated using the protocol described by Ye et al. (2016). The aliquots (0.2 mL) of each solution were examined at 0, 5, 10, 20, 30, 60, 90, 120, 150, 200, and 250 min for the measuring of released glucose using GOD-POD assay kit.

2.11 | Digestion model

The following digestive models Equations (8)–(12) were used to describe the digestogram (Nguyen & Sopade, 2018):

1. First-order kinetics

$$D_t = D_\infty(1 - \exp[-K_1 t]), \tag{8}$$

where D_t is the digested starch expressed as g/100 g at time t in min, K_1 is the rate of digestion in min^{-1}, and D_∞ is the maximum digestible starch in g/100 g.

2. Michaelis–Menten model

$$-\frac{dS}{dt} = \frac{dP}{dt} = \frac{V_{max}S}{K_M + S}, \tag{9}$$

where V_{max} is the maximum digestion velocity of the reaction (mg min^{-1} mL^{-1}), K_M is Michaelis–Menten digestion rate constant (mg/mL), S is the substrate concentration (mg/mL), and P is the product concentration (mg/mL).

3. Paolucci Jeanjean model

$$D_t = \frac{At^2}{B^2 + t^2}, \tag{10}$$

where A is maximum digestible starch expressed as g/100 g and B is rate of digestion in min^{-1}.

4. Logistic model

$$D_t = \frac{D_\infty}{1 + \left(\frac{D_\infty}{D_0} - 1\right)\exp(-K_2 t)}, \tag{11}$$

where D_0 is the initial digestible starch in g/100 g, D_∞ is the maximum digestible starch in g/100 g, and K_2 is the logistic model constant.

5. Weibull model

$$D_t = D_\infty + (D_0 - D_\infty)\exp\left(-[K_3 t]^\beta\right), \tag{12}$$

where D_0 is the initial digestible starch in g/100 g, D_∞ is the maximum digestible starch in g/100 g, K_3 is Weibull model constant, and β is shape constant.

2.12 | Statistical analysis

All the experiments were performed in triplicate and the reported results were average values of the triplicates with standard deviation. One-way analysis of variance (ANOVA) was accomplished at a 5 % level of significance using IBM SPSS software Chicago, IL, USA 22 version. Duncan's multiple comparison test and Tukey's HSD test was performed to receive the significance level ($p \leq 0.05$).

3 | RESULTS AND DISCUSSIONS

3.1 | Functional properties

The WAC and SP of native and modified EFYS are shown in Table 1. The different values of WAC and SP of the native and modified starches showed that each kind of starch swells in different ways demonstrating different molecular orientation within granules. Both the treatments enhanced WAC and SP which varied significantly ($p \leq 0.05$), denoting 0.68 ± 0.02 g/g for US EFYS and in the range of 0.73 ± 0.02 to 0.76 ± 0.02 g/g for US-AL treatment. The highest values of WAC (0.76 ± 0.02 g/g) and SP (13.02 ± 0.04 g/g) were observed for the sample treated with US-AL45, as compared to the native EFYS and other modified EFYS. According to Wang et al. (2020), physical damage of starch granules and an increase in the amorphous phase are the possible reasons for increasing the WAC and SP in US EFYS. The highest increase in amylose content was observed in US-AL45 EFYS (~10.02 ± 0.08 %) as compared to native (~22.77 ± 0.98 %), US (~25.33 ± 0.35 %), US-AL15 (~26.32 ± 0.47 %), and US-AL30 (~27.10 ± 0.21 %) EFYS. The enhancement of amylose content in US and US-AL EFYS promoted the increase in WAC and SP. The

TABLE 1 Functional properties of native and US-AL EFYS

Samples	Water absorption capacity (g/g)	Swelling power (g/g)	Solubility (%)	Amylose (%)	Whiteness index
Native EFYS	0.60 ± 0.02[a]	8.7 ± 0.28[a]	7.37 ± 0.37[a]	22.77 ± 0.98[a]	93.49 ± 0.94[a]
US EFYS	0.68 ± 0.02[b]	10.47 ± 0.42[b]	8.6 ± 0.24[b]	25.33 ± 0.35[b]	92.22 ± 0.84[a]
US-AL15 EFYS	0.73 ± 0.02[b,c]	11.62 ± 0.29[c]	9.4 ± 0.29[c]	26.32 ± 0.47[b,c]	90.40 ± 0.66[b]
US-AL30 EFYS	0.75 ± 0.03[c]	12.64 ± 0.24[d]	9.56 ± 0.16[c,d]	27.10 ± 0.15[c]	88.41 ± 0.77[c]
US-AL45 EFYS	0.76 ± 0.02[c]	13.02 ± 0.04[d]	10.02 ± 0.08[d]	27.35 ± 0.21[c]	87.71 ± 0.33[c]

Note: Values with different superscripts in the same column are significantly different ($p \leq 0.05$) by Duncan's HSD test.
Abbreviations: EFYS, elephant foot yam starch; US, ultrasoication; US-AL15, ultrasonication pretreated autoclave with 15 min; US-AL30, ultrasonication pretreated autoclave with 30 min; US-AL45, ultrasonication pretreated autoclave with 45 min.

increase in hydrophilic groups is the probable reason for increasing the WAC and SP with an increase in US pretreated AL treatment time (Sujka & Jamroz, 2013). US along with AL treatment enhanced the WAC and SP compared to US treatment alone. This can be due to the more binding of free hydroxyl groups of starch and water molecules through hydrogen bonding and enhances the WAC of starch (Deka & Sit, 2016; Sujka & Jamroz, 2013). The significant ($p \leq 0.05$) increase in amylose content was observed to 25.33 ± 0.35 % for US and in the range of 26.32 ± 0.47 to 27.35 ± 0.21 % for US-AL treatment, as compared to the native EFYS (~22.77 ± 0.98 %). Another possible reason for increasing the swelling properties in US-AL treatment could be due to the occurring of granular fusion which accelerated the number of longer amylopectin chains and increased the number of available hydroxyl groups leading to the increase in WAC and SP of US and US-AL treated EFYS (Deka & Sit, 2016). The findings were also supported by Wang et al. (2020), where significant increment in swelling properties was observed in US modified sweet potato starch.

The increase in solubility of US and US-AL EFYS is presented in Table 1. The modification treatments enhanced SL significantly ($p \leq 0.05$) varied 8.6 ± 0.24 % for US EFYS and in the range of 9.4 ± 0.2 % to 10.02 ± 0.08 % for US-AL treatment, as compared to native EFYS (7.37 ± 0.37 %). Similar findings were reported by Lima and Andrade (2010), where increase in solubility was observed in ultrasonic treated high amylose maize starch. US treatment enhances the mobility of amylose chains and US-AL treatment further accelerates the hydration performance of EFYS resulting in increasing solubility (Deka & Sit, 2016; Sujka & Jamroz, 2013). The increased solubility caused by US and US-AL may be due to an increase in amylose content, which aids in amylose dissolution and granular fusion, and increases the availability of more exposed hydroxyl groups.

3.2 | Whiteness index (WI)

The WI of native and modified EFYS are presented in Table 1. The significant ($p \leq 0.05$) reduction in WI was observed which varied 92.22 ± 0.84 for US and in the range of 90.40 ± 0.66 to 87.71 ± 0.33 for US-AL treatment, as compared to native EFYS (93.49 ± 0.94). It is noteworthy to state that, US treatment preserved the WI of EFYS. The reduction in WI was observed with increasing US

pre-treated AL treatment time and US-AL45 showed the highest decrement in WI to 87.71 ± 0.33. Similar results were reported when taro starch was treated in autoclave (Deka & Sit, 2016). The reduction in WI can be due to Millard reaction occurring between reducing sugars from starch and the protein contents in present samples during modification. Another reason for reduction in WI for US-AL treatments with varying time can be due to the application of extreme temperature, pressure, and longer duration of treatment time which can promote breakdown of starch into simple sugars known as caramelization reactions (Miranda, Maureira, Rodriguez, & Vega-Gálvez, 2009). As the severity of US treatment was less than that of US-AL treatment, the alteration in WI from that of native starch was found to be less for the starches treated in US compared to starches treated in US-AL.
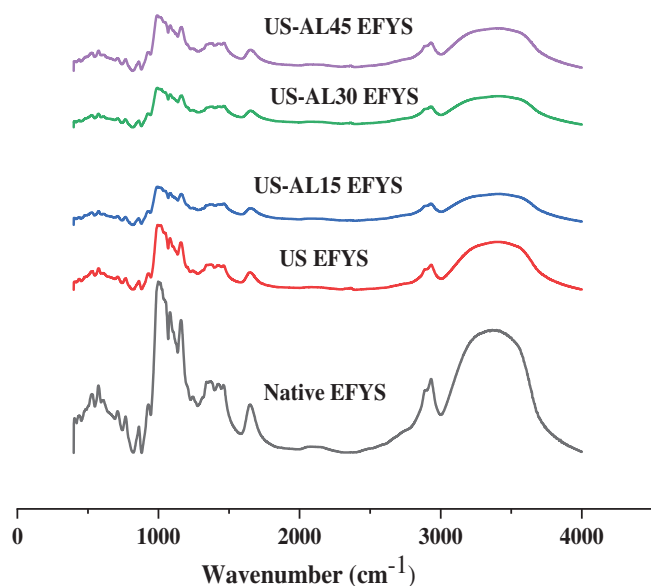
3.3 | Granular morphology

Scanning electron micrographs (2.00 KX) for native and modified EFYS is presented in Figure 1. It was noticed that native EFYS contained a mixture of starch granules of different shapes and sizes. The shape of starch granules include spheres, ellipses, and polygons (Figure 1a). Majorly smooth surface was observed in native EFYS granules, which exhibited in scattered or separated entities with slight to not at all clustering. Presence of any cracks, pores and channels were not observed on granular surface after modification. Nevertheless, few granular surfaces showed little contortion as designated by arrows (Figure 1a). The above results are analogous with those attained by Sukhija et al. (2016a, 2016b), and Nagar et al. (2019). US treatment increased the inter granular spaces of the starch (Figure 1b) and hence accelerated enzymatic hydrolysis. Implementing US-assisted AL treatment caused the disintegration of big clusters into smaller ones and enhanced surface contortion. Interestingly, loss of granular integrity increased with increase in AL treatment time. US-AL45 showed the highest granular aggregation and restricted the available surface areas for the binding of enzyme and stimulated the increase in RS content. Conclusively, US treatment solely was able to increase the inter-granular spaces of starch, while treating under high steam pressure in AL accelerated the electrostatic forces between water molecules and starch particles causing particle agglomerations (Bet et al., 2018).
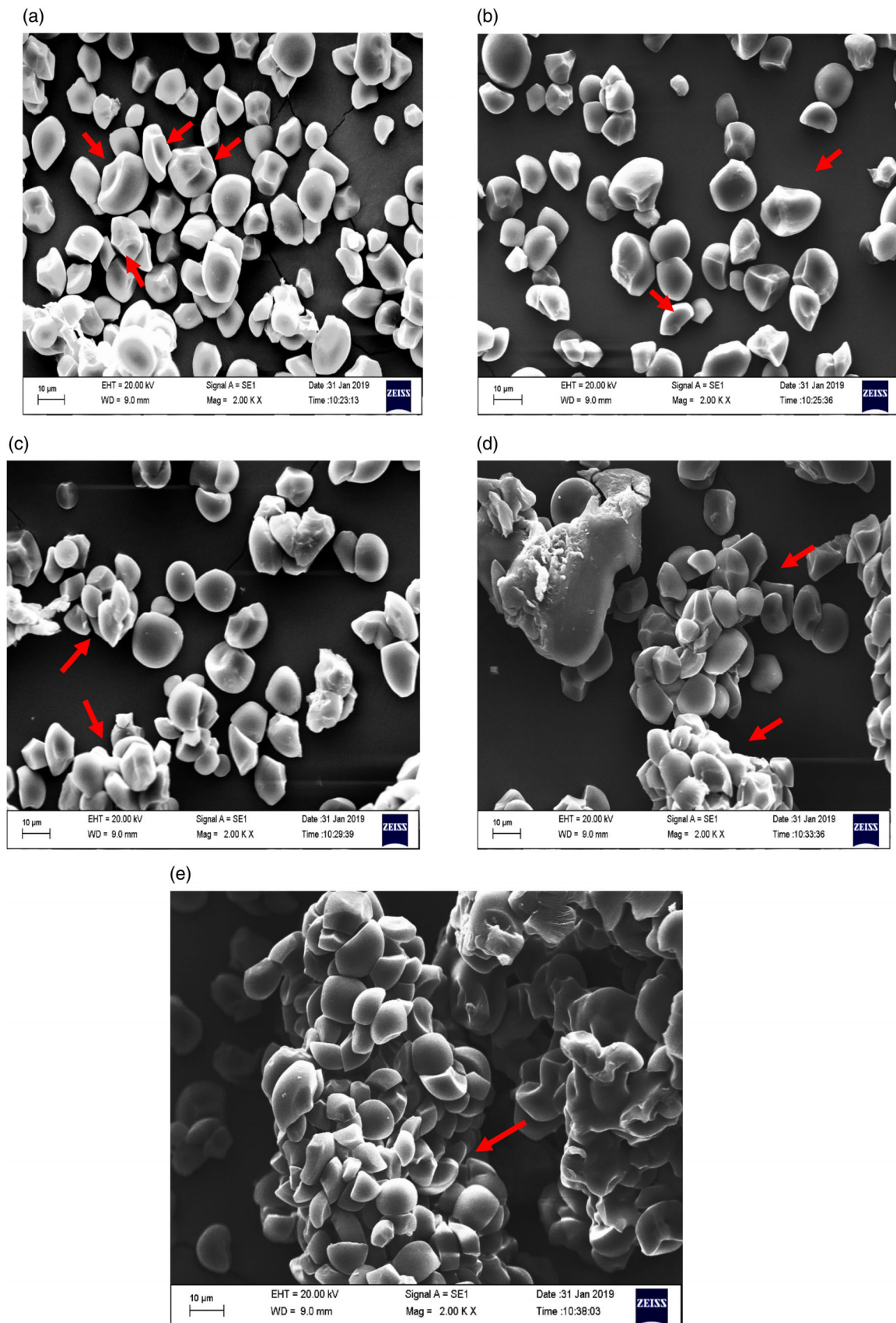
FIGURE 1 SEM micrographs of native and modified elephant foot yam starch (EFYS) granules. (a) Native EFYS, (b), US EFYS, (c) US-AL15 EFYS, (d) US-AL30 EFYS, and (e) US-AL45 EFYS

3.4 | Functional group analysis

The FTIR spectrums of native and modified EFYS are shown in Figure 2. Strong absorption bands at 1010.05 cm^{-1} and several slight absorption bands were noted at the range of 900–400 cm^{-1} attributable to C-H bending causing skeletal vibration of glucose pyranose ring (Bai, Hébraud, Ashokkumar, & Hemar, 2017). Similar results were noted in normal potato and waxy potato starch (Bai et al., 2017). It is noteworthy to state that the infrared bands at 1047 and 1022 cm^{-1} were found to be associated with ordered and amorphous starch structures, respectively (Zeng, Ma, Kong, Gao, & Yu, 2015). The amount of ordered starch to amorphous starch is expressed by the ratio of band heights at 1047 and 1022 cm^{-1}. The 1047/1022 ratio maintained the following order among native and modified EFYS: US-AL45 > US-AL30 > US-AL15 > native > US. Figure 2 suggests that the ratio 1047/1022 increased in US-AL45 treated EFYS, but decreased in US treatment. The higher ratio indicates that the presence of moisture content and thermal energy during AL treatment cause more effective packing of double helices within the crystalline lamella (Chung, Hoover, & Liu, 2009). Additional weak C-H stretching vibration was observed at approximately 2932.28 and 2894.19 cm^{-1}. Furthermore, two weak absorption bands were noticeable at 1366.34 and 1460.35 cm^{-1} due to the cumulative vibrations of O-H plane bending with C-H oscillations. The intensity of C-H and O-H vibrations were found to decrease in modified EFYS (US-AL45 < US-AL 30 < US-AL 15 < US) as compared to native EFYS. The reduction in broad absorption band in the range of 3,300–3,600 cm^{-1} was observed in US pretreated AL EFYS that indicated the less presence of O-H stretching in polymeric arrangement of starch particles as compared to native EFYS. A sensible absorption of a band because of unconjugated C=C linear alkene was observed at 1650.31 cm^{-1} which also showed reduction in the order native < US-AL45 < US-

AL30 < US-AL15 < US EFYS. Finally, the highest intensity reduction in C-CO-C stretching and bending (1081.405 cm^{-1}) was detected in US-AL45 as compared to native and other modified EFYS. A visual assessment showed the differences in absorbency observed in US and US-AL EFYS. Major absorption bands are consistent with varying intensity in the modified EFYS. The reduction in peak intensity in US-AL EFYS was observed at 1000–1010.05 cm^{-1} indicating the breakdown of C-H bonding. However, the increase in molecular integrity, recombination of amylose–amylose and amylose–amylopectin interactions with hydrogen bond were responsible for the reduction in absorption bands which was noticed in US and US-AL treated EFYS (Chang, Lu, Bian, Tian, & Jin, 2021). It is important to note that all the modified EFYS showed similar spectra with its native counterpart suggesting that no further formation of new functional groups.

## 3.5 | *In vitro* digestibility

In vitro starch digestibility of native and modified EFYS is presented in Table 2. Highest increase in RS was observed in US-AL45 EFYS (39.13 ± 1.19 %) as compared to native EFYS (30.65 ± 1.06 %) and other modified (US, US-AL15, and US-AL30) EFYS. It is interesting to note that US treatment alone decreased the RS, and SDS content significantly ($p ≤ 0.05$) up to 24 ± 0.26 % and 6.90 ± 0.58 %, respectively, as compared to US-assisted AL treatments. The pressure generated during US treatment was responsible for the disruption of the starch's internal structure, driving to the reduction in granular integrity and more prominent susceptibility to enzymatic hydrolysis (Chang et al., 2021). The loss of granular integrity was observed in US EFYS (Figure 1b) and hence supported the increase in enzyme attack. The increase in enzyme susceptibility was also reported by Kunyanee and Luangsakul (2020) for US-treated rice starch. Moreover, US treatment induced the formation of amylose content (Table 1) attributing to the increase in amorphous phase which is highly available for enzymes. US-AL treatment significantly ($p ≤ 0.05$) increased the SDS and RS content, which varied in the range 15.06 ± 1.23 % to 13.73 ± 1.04 % and 32.91 ± 2.50 to 39.13 ± 1.19 %, respectively, as compared to native counterpart 9.13 ± 0.75 % and 30.65 ± 1.06 % for SDS and RS, respectively. The enhancement of SDS and RS content in US-AL EFYS could be due to the formation of compact granular structures (Figure 1c–e) and increased interactions between short amylose–short amylose caused resistant to enzymatic digestion (Chang et al., 2021). The finding is consistent with the FTIR analysis, which revealed an improvement in ordered structure for US-AL45 followed by US-AL30 > US-AL15 > native > US EFYS. The molecular schematic representation of native and modified EFYS is shown in Figure 3 which depicts the production of short amylose from the end of amylopectin chains during US treatment. However, US-AL treatment accelerated the formation of short amylose crystals which was found to be highest in US-AL45 treatment and acted as barriers against enzyme attack, resulting in the formation of the highest RS fraction. The results were supported by a study where slower digestion rate was observed in US pretreated debranched waxy maize starch (Chang et al., 2021).

FIGURE 2 FTIR analysis of native and modified EFYS

Samples	Readily digestible starch (%)	Slowly digestible starch (%)	Resistant starch (%)
Native EFYS	59.30 ± 0.58^a	9.13 ± 0.75^a	30.65 ± 1.06^a
US EFYS	68.18 ± 0.72^b	6.90 ± 0.58^b	24 ± 0.26^b
US-AL15 EFYS	51.11 ± 1.45^c	15.06 ± 1.23^c	32.91 ± 2.50^a
US-AL30 EFYS	47.66 ± 1.02^d	14.92 ± 0.64^c	36.5 ± 1.45^c
US-AL45 EFYS	46.22 ± 1.51^d	13.73 ± 1.04^c	39.13 ± 1.19^c

Note: Values with different superscripts in the same column are significantly different ($p < 0.05$) by Duncan's HSD test.

Abbreviations: EFYS, elephant foot yam starch; US, ultrasoication; US-AL15, ultrasonication pretreated autoclave with 15 min; US-AL30, ultrasonication pretreated autoclave with 30 min; US-AL45, ultrasonication pretreated autoclave with 45 min.
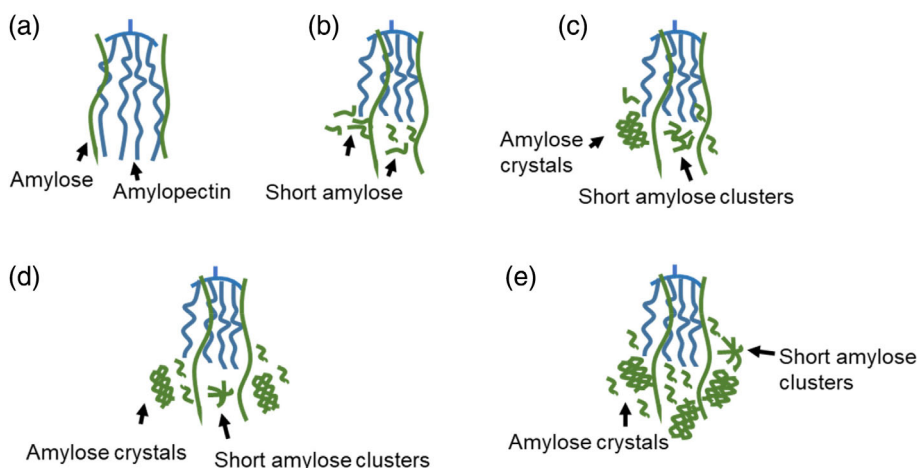
FIGURE 3 Molecular schematic representation of (a) native EFYS, (b) US EFYS, (c) US-AL15 EFYS, (d) US-AL30 EFYS, and (e) US-AL45 EFYS

However, with the increase in AL treatment time imparts positive impact on increasing the RS and SDS content of US-AL EFYS.

3.6 | Digestogram modeling

Different mathematical and empirical kinetic models were employed to study the digestogram modeling of native and modified EFYS (Figure 4). The Michaelis–Menten model is considered to be the most commonly used mathematical model for starch digestogram. Significant ($p \leq 0.05$) reduction was observed in V_{max} for US-AL45 EFYS to 61.22 ± 1.62 mg min^{-1} mL^{-1} shows the highest decrease in enzyme velocity within starch granules as compared to native EFYS containing 88.94 ± 1.66 mg min^{-1} mL^{-1} and other US-AL modified EFYS varying the range from 71.92 ± 2.14 to 82.51 ± 1.36 mg min^{-1} mL^{-1}, respectively. Interestingly, an increase in V_{max} to 92.56 ± 1.26 mg min^{-1} mL^{-1} was noted in EFYS while treating with US. The increase in V_{max} in US-treated EFYS can be due to the pressure generation during US treatment that disrupts the granular integrity (Figure 1b) and accelerates the enzyme penetration within granules. For practical purposes, K_m is the concentration of the substrate which permits the enzyme to achieve half V_{max}. An enzyme with a high K_m has a low affinity for its substrate and requires a greater concentration of the substrate to achieve V_{max}. So, it indicates that the lower the K_M value, the higher the affinity of the enzyme for the substrate. The study shows the decrease in K_M value in US EFYS ~4.12 ± 0.41 mg/mL and US-AL EFYS which varied in the range ~2.55 ± 0.60 to 4.34 ± 0.52 mg/mL as compared to native EFYS (4.71 ± 0.61 mg/mL). The increased amylose content in US and US-AL EFYS could improve the substrate's affinity for the enzyme hydrolysis. Considering the computational simplicity, the first-order model is widely implemented to express starch the digestogram process and document the decrease in D_∞ for US-AL EFYS which varied in the range ~58.64 ± 1.14 to 78.21 ± 0.76 g/100 g, as compared to native EFYS ~84.26 ± 0.54 g/100 g. A significant increase in D_∞ was noted in US-treated EFYS and reported as 88.07 ± 0.72 g/100 g. Similarly, Paolucci Jeanjean, Logistic, and Weibull models show the similar trend of reduction in maximum digested starch (A for Paolucci Jeanjean; $D_{\infty Logistic}$; $D_{\infty Weibull}$, respectively) in US-AL EFYS and increment in the same was observed in EFYS when treated with only US treatment. The rate of digestion for all the models (B: Paolucci Jeanjean; K_1: first-order kinetics; K_2: Logistic; K_3: Weibull model) show the highest decrease in US-AL45 EFYS. In comparison to native, US-AL15, and US-AL30 EFYS, the increase in D_∞ was observed in US EFYS for all the models that indicated a higher susceptibility to enzyme hydrolysis, while US-AL45 EFYS was found to be more resistant against enzyme
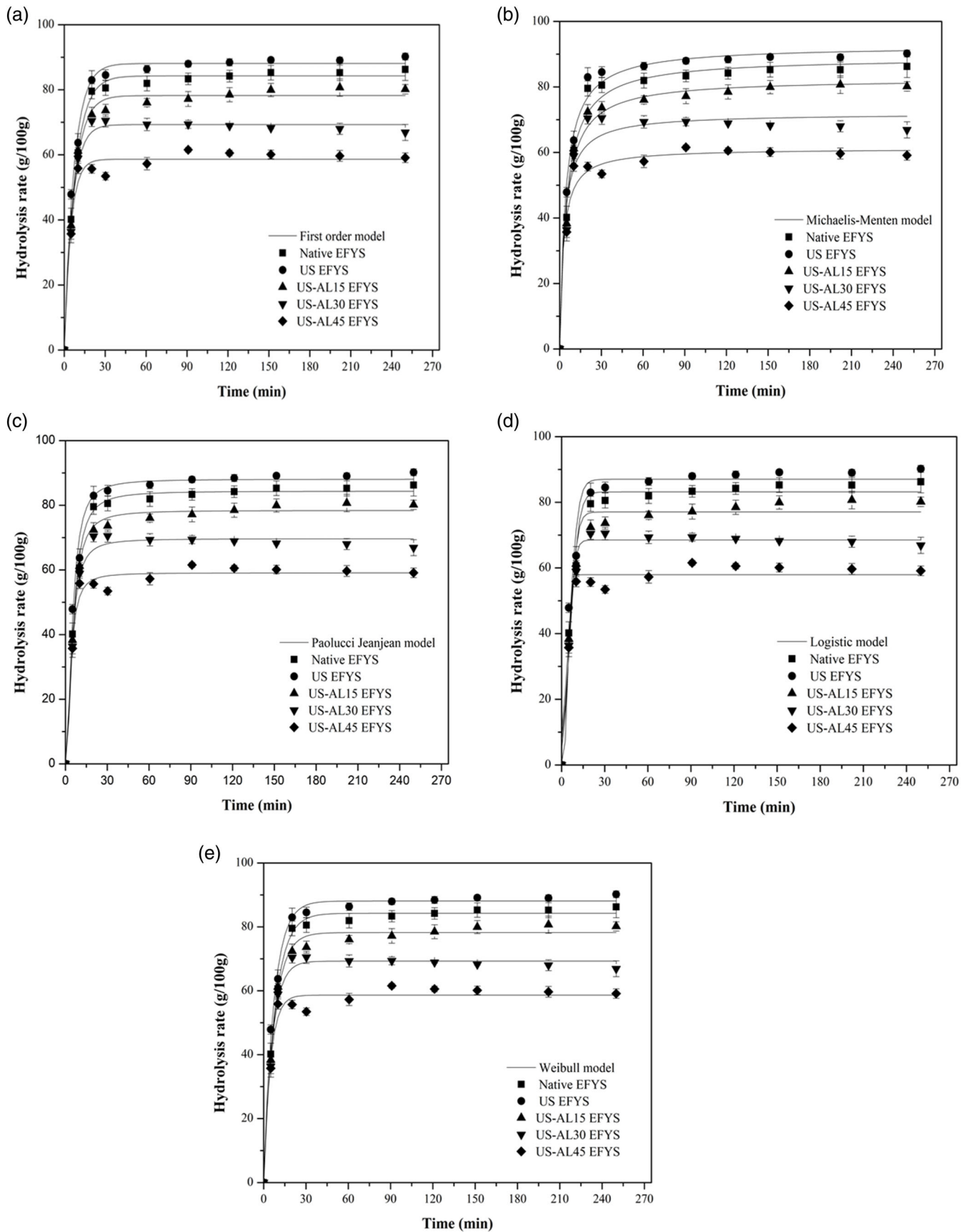
FIGURE 4 Digestogram of native, ultrasonic, ultrasonic pretreated autoclave modified with 15, 30, 45 min treatment: (a) first-order kinetics model, (b) Michaelis–Menten model, (c) Paolucci Jeanjean model, (d) Logistic model, and (e) Weibull model

TABLE 3 Digestogram modeling of native and modified EFYS

First-order kinetics

	D_0	K_1	Adj. R^2
Native EFYS	84.26 ± 0.54^b	0.129 ± 0.004^c	0.997
US EFYS	88.07 ± 0.72^a	0.141 ± 0.006^{bc}	0.995
US-AL15 EFYS	78.21 ± 0.76^c	0.140 ± 0.007^{bc}	0.993
US-AL30 EFYS	69.29 ± 0.76^d	0.169 ± 0.011^b	0.990
US-AL45 EFYS	58.64 ± 1.14^e	0.210 ± 0.026^a	0.975
		Average	0.990

Michaelis–Menten model

	V_{max}	K_M	Adj. R^2
Native EFYS	88.94 ± 1.66^a	4.71 ± 0.61^a	0.983
US EFYS	92.56 ± 1.26^a	4.12 ± 0.41^{ab}	0.990
US-AL15 EFYS	82.51 ± 1.36^b	4.34 ± 0.52^{ab}	0.986
US-AL30 EFYS	71.92 ± 2.14^c	3.07 ± 0.78^b	0.951
US-AL45 EFYS	61.22 ± 1.62^d	2.55 ± 0.60^{bc}	0.967
		Average	0.975

Paolucci Jeanjean model

	A	B	Adj. R^2
Native EFYS	84.37 ± 0.69^b	5.57 ± 0.21^a	0.995
US EFYS	88.07 ± 1.02^a	5.05 ± 0.28^{ab}	0.989
US-AL15 EFYS	78.41 ± 0.59^c	5.22 ± 0.18^{ab}	0.995
US-AL30 EFYS	69.65 ± 0.77^d	4.56 ± 0.25^b	0.990
US-AL45 EFYS	59.10 ± 1.02^e	3.82 ± 0.36^c	0.980
		Average	0.989

Logistic model

	D_∞	K_2	D_0	Adj. R^2
Native EFYS	83.17 ± 1.72^b	0.340 ± 0.063^a	8.96 ± 0.33^{ab}	0.968
US EFYS	87.01 ± 2.17^a	0.345 ± 0.078^a	10.78 ± 0.46^a	0.951
US-AL15 EFYS	77.04 ± 1.58^c	0.403 ± 0.080^a	7.14 ± 3.13^{ab}	0.967
US-AL30 EFYS	68.52 ± 0.97^d	0.513 ± 0.090^a	4.76 ± 2.10^{bc}	0.983
US-AL45 EFYS	57.93 ± 0.98^e	0.976 ± 0.762^a	0.69 ± 0.02^c	0.978
			Average	0.969

Weibull model

	D_∞	K_3	D_0	Adj. R^2
Native EFYS	84.26 ± 0.58^b	0.129 ± 0.005^c	0.022 ± 0.007^e	0.996
US EFYS	88.09 ± 0.76^a	0.139 ± 0.007^{bc}	0.831 ± 0.009^a	0.994
US-AL15 EFYS	78.21 ± 0.81^c	0.140 ± 0.009^{bc}	0.094 ± 0.002^d	0.992
US-AL30 EFYS	69.28 ± 0.80^d	0.170 ± 0.012^b	0.795 ± 0.002^b	0.989

TABLE 3 (Continued)

Weibull model

	D_∞	K_3	D_0	Adj. R^2
US-AL45 EFYS	58.64 ± 1.21^e	0.212 ± 0.029^a	0.380 ± 0.003^c	0.972
			Average	0.988

Note: Values with different superscripts in the same column are significantly different ($p < 0.05$) by Tukey's HSD test.

Abbreviations: EFYS, elephant foot yam starch; HAO, hot air oven; AL, autoclave; MW, microwave; D_0, initial digested starch in g/100 g; K_1, digestion rate constant for first-order kinetics model; V_{max}, maximum digestion velocity in mg $\min^{-1}$ mL^{-1}; K_M, Michaelis–Menten digestion rate constant in mg/mL; A, maximum digestible starch in Paolucci Jeanjean model expressed as g/mL; B, rate of enzyme digestion in $\min^{-1}$; D_∞, maximum digestible starch in g/100 g; K_2, logistic model constant; K_3, Weibull model constant.

attack. The development of short amylose from the end of amylopectin chains could form ordered structures and short crystals that may act as a resistance against enzyme attack and lead to the reduction in D_∞. In addition, the formation of the particle aggregates accelerated when the treatment time of US-AL modification was increased. Another possible reason for the highest reduction in D_∞ in US-AL45 for all the models could be due to the formation of highest particle agglomerations (Figure 1e) that decreased the available surface area for the binding sites of enzymes. Tester, Karkalas, and Qi (2004) stated that the larger granules comprise of smaller surface area to volume ratio that can help to reduce the potential enzyme attack. The density of starch particles prevails in US-AL15, US-AL30, US-AL45 EFYS exhibited in lowering down the digestion rate and the highest decrease of that predominates in US-AL45 EFYS. Barua, Rakshit, and Srivastav (2021) also studied digestogram modeling of heat moisture treated EFYS and reported similar trend of reduction in D_∞ for all the modified EFYS using first-order kinetics, Paolucci Jeanjean, Logistic, and Waliszweski models. Table 3 summarizes the adjusted coefficient of determination (R^2_{Adj}) for the first-order kinetics model ranged from 0.975–0.997, 0.951–0.99 for Michaelis–Menten model, 0.98–0.995 for Paolucci Jeanjean, 0.951–0.983 for logistic model, and 0.972–0.996 for Weibull model. However, considering the average R^2_{Adj} which was > 0.9 for all the models displayed suitable fitting of the experimental data with the model predicted values.

4 | CONCLUSIONS

The effect of the dual modification treatments using US and US pretreated AL on the functional, morphological, and digestion properties of EFYS has been investigated in this study. The effect of US and US-AL treatment was pronounced in morphology of EFYS. US-AL treatment was responsible for the formation of particle aggregation which further facilitated in reduction of enzyme attacks. In the other way, US treatment was able to break down the starch aggregation

which was observed in native counterpart and accelerated the enzyme hydrolysis. FTIR analysis exhibited the increase in the amount of ordered to amorphous starch ratio ($1047/1022 \, cm^{-1}$) in US-AL45 followed by US-AL30, US-AL15, native, and US EFYS. However, FTIR analysis revealed no variations in peak shifting, indicating that the US and US-AL treatments failed to encourage the new bond formation. US treatment was able to preserve the WI of EFYS whereas reduction in WI was noted in US-AL EFYS. Both the treatments were able to increase WAC, SP, and SL of EFYS. It is interesting to state that increasing the treatment time during US-AL treatment helps in reducing the digestion rate. So the effect of US-AL45 was found to be more effective on reducing the rate of digestion as compared to the samples only treated with US. US pretreatment was found to be effective in the production of short amylose at the end of amylopectin chains which further formed short ordered crystals resulting in the reduction of the rate of digestion in US-AL EFYS. The digestogram modeling of native and modified (US, US-AL15, US-AL30, and US-AL45) EFYS was conducted using the first-order kinetics, Michaelis–Menten, Paolucci Jeanjean, Logistic, and Weibull models and all the models were found to be suitable ($R^2_{Adj} > 0.9$) for fitting the digestogram data of native and modified EFYS. The induced properties of these starches after modification can be definitely beneficial in formulating food products for diabetes and obese patients. Modified EFYS can be used as thickening, gelling, and enhancing agents in bakery products, as well as in the preparation of low digestible noodles and pasta for diabetes and obese patients. The study indicated the importance of using the green technology, namely US pretreated autoclave treatment in modifying the functional and digestion qualities of EFYS that can be scaled up further for industrial applications.

ACKNOWLEDGMENTS

CONFLICT OF INTEREST

The authors declare no potential conflict of interest.

AUTHOR CONTRIBUTIONS

Sreejani Barua: Conceptualization; investigation; data curation; methodology; visualization; software; writing – original draft. **Karan Tudu**: Investigation; data curation; software; visualization; formal analysis. **Madhulekha Rakshit**: Software; methodology; writing – review and editing. **Prem Prakash Srivastav**: Supervision.

DATA AVAILABILITY STATEMENT

Research data are not shared.

ORCID

Sreejani Barua https://orcid.org/0000-0002-9681-4898
Madhulekha Rakshit https://orcid.org/0000-0003-4113-573X
Prem Prakash Srivastav https://orcid.org/0000-0002-6676-1289

REFERENCES

Babu, A. S., & Parimalavalli, R. (2013). Effect of autoclaving on functional, chemical, pasting and morphological properties of sweet potato starch. *Journal of Root Crops*, 39(1), 78–83.

Bai, W., Hébraud, P., Ashokkumar, M., & Hemar, Y. (2017). Investigation on the pitting of potato starch granules during high frequency ultrasound treatment. *Ultrasonics Sonochemistry*, 35, 547–555. https://doi.org/10.1016/j.ultsonch.2016.05.022

Barua, S., & Srivastav, P. P. (2017). Effect of heat-moisture treatment on resistant starch functional and thermal properties of mung bean (*Vigna radiate*) starch. *Journal of Nutritional Health & Food Engineering*, 7(4), 248. https://doi.org/10.15406/jnhfe.2017.07.00248

Barua, S., Khuntia, A., Srivastav, P. P., & Vilgis, T. A. (2021). Understanding the native and hydrothermally modified elephant foot yam (*Amorphophallus paeoniifolius*) starch system: A multivariate approach. *LWT*, 150, 111958. https://doi.org/10.1016/j.lwt.2021.111958

Barua, S., Rakshit, M., & Srivastav, P. P. (2021). Optimization and digestogram modeling of hydrothermally modified elephant foot yam (*Amorphophallus paeoniifolius*) starch using hot air oven, autoclave, and microwave treatments. *LWT*, 145, 111283. https://doi.org/10.1016/j.lwt.2021.111283

Bet, C. D., de Oliveira, C. S., Colman, T. A. D., Marinho, M. T., Lacerda, L. G., Ramos, A. P., & Schnitzler, E. (2018). Organic amaranth starch: A study of its technological properties after heat-moisture treatment. *Food Chemistry*, 264, 435–442. https://doi.org/10.1016/j.foodchem.2018.05.021

Chang, R., Lu, H., Bian, X., Tian, Y., & Jin, Z. (2021). Ultrasound assisted annealing production of resistant starches type 3 from fractionated debranched starch: Structural characterization and in-vitro digestibility. *Food Hydrocolloids*, 110, 106141. https://doi.org/10.1016/j.foodhyd.2020.106141

Chung, H. J., Hoover, R., & Liu, Q. (2009). The impact of single and dual hydrothermal modifications on the molecular structure and physicochemical properties of normal corn starch. *International Journal of Biological Macromolecules*, 44(2), 203–210. https://doi.org/10.1016/j.ijbiomac.2008.12.007

Deka, D., & Sit, N. (2016). Dual modification of taro starch by microwave and other heat moisture treatments. *International Journal of Biological Macromolecules*, 92, 416–422. https://doi.org/10.1016/j.ijbiomac.2016.07.040

Dundar, A. N., & Gocmen, D. (2013). Effects of autoclaving temperature and storing time on resistant starch formation and its functional and physicochemical properties. *Carbohydrate Polymers*, 97(2), 764–771. https://doi.org/10.1016/j.carbpol.2013.04.083

Hu, A., Lu, J., Zheng, J., Sun, J., Yang, L., Zhang, X., & Lin, Q. (2013). Ultrasonically aided enzymatical effects on the properties and structure of mung bean starch. *Innovative Food Science & Emerging Technologies*, 20, 146–151. https://doi.org/10.1016/j.ifset.2013.08.005

Jagannadham, K., Parimalavalli, R., & Babu, A. S. (2014). Effect of autoclaving on chemical, functional and morphological properties of chickpea (*Cicer arietinum* L.) Starch. *International Interdisciplinary Research Journal*, 4, 284–294.

Kunyanee, K., & Luangsakul, N. (2020). The effects of ultrasound-assisted recrystallization followed by chilling to produce the lower glycemic index of rice with different amylose content. *Food Chemistry*, 323, 126843. https://doi.org/10.1016/j.foodchem.2020.126843

Li, M., Li, J., & Zhu, C. (2018). Effect of ultrasound pretreatment on enzymolysis and physicochemical properties of corn starch. *International Journal of Biological Macromolecules*, 111, 848–856. https://doi.org/10.1016/j.ijbiomac.2017.12.156

Lima, F. F., & Andrade, C. T. (2010). Effect of melt-processing and ultrasonic treatment on physical properties of high-amylose maize starch. *Ultrasonics Sonochemistry*, *17*(4), 637–641. https://doi.org/10.1016/j.ultsonch.2010.01.001

McGrance, S. J., Cornell, H. J., & Rix, C. J. (1998). A simple and rapid colorimetric method for the determination of amylose in starch products. *Starch-Stärke*, *50*(4), 158–163. https://doi.org/10.1002/(SICI)1521-379X(199804)50:4<158::AID-STAR158>3.0.CO;2-7

Miranda, M., Maureira, H., Rodriguez, K., & Vega-Gálvez, A. (2009). Influence of temperature on the drying kinetics, physicochemical properties, and antioxidant capacity of *Aloe Vera* (*Aloe Barbadensis* miller) gel. *Journal of Food Engineering*, *91*(2), 297–304. https://doi.org/10.1016/j.jfoodeng.2008.09.007

Nagar, M., Sharanagat, V. S., Kumar, Y., Singh, L., & Mani, S. (2019). Influence of xanthan and agar-agar on thermo-functional, morphological, pasting and rheological properties of elephant foot yam (*Amorphophallus paeoniifolius*) starch. *International Journal of Biological Macromolecules*, *136*, 831–838. https://doi.org/10.1016/j.ijbiomac.2019.06.133

Nattapulwat, N., Purkkao, N., & Suwithayapan, O. (2009). Preparation and application of carboxymethyl yam (*Dioscorea esculenta*) starch. *AAPS PharmSciTech*, *10*(1), 193–198. https://doi.org/10.1208/s12249-009-9194-5

Nguyen, G. T., & Sopade, P. A. (2018). Modeling starch digestograms: Computational characteristics of kinetic models for in vitro starch digestion in food research. *Comprehensive Reviews in Food Science and Food Safety*, *17*(5), 1422–1445. https://doi.org/10.1111/1541-4337.12384

Singh, R., & Sharanagat, V. S. (2020). Physico-functional and structural characterization of ultrasonic-assisted chemically modified elephant foot yam starch. *International Journal of Biological Macromolecules*, *164*, 1061–1069. https://doi.org/10.1016/j.ijbiomac.2020.07.185

Sujka, M., & Jamroz, J. (2013). Ultrasound-treated starch: SEM and TEM imaging, and functional behaviour. *Food Hydrocolloids*, *31*(2), 413–419. https://doi.org/10.1016/j.foodhyd.2012.11.027

Sukhija, S., Singh, S., & Riar, C. S. (2016a). Effect of oxidation, cross-linking and dual modification on physicochemical, crystallinity, morphological, pasting and thermal characteristics of elephant foot yam (*Amorphophallus paeoniifolius*) starch. *Food Hydrocolloids*, *55*, 56–64. https://doi.org/10.1016/j.foodhyd.2015.11.003

Sukhija, S., Singh, S., & Riar, C. S. (2016b). Isolation of starches from different tubers and study of their physicochemical, thermal, rheological and morphological characteristics. *Starch-Stärke*, *68*(1–2), 160–168. https://doi.org/10.1002/star.201500186

Tester, R. F., Karkalas, J., & Qi, X. (2004). Starch structure and digestibility enzyme-substrate relationship. *World's Poultry Science Journal*, *60*(2), 186–195. https://doi.org/10.1079/WPS200312

Wang, H., Xu, K., Ma, Y., Liang, Y., Zhang, H., & Chen, L. (2020). Impact of ultrasonication on the aggregation structure and physicochemical characteristics of sweet potato starch. *Ultrasonics Sonochemistry*, *63*, 104868. https://doi.org/10.1016/j.ultsonch.2019.104868

Wani, I. A., Hamid, H., Hamdani, A. M., Gani, A., & Ashwar, B. A. (2017). Physico-chemical, rheological and antioxidant properties of sweet chestnut (*Castanea sativa* Mill.) as affected by pan and microwave roasting. *Journal of Advanced Research*, *8*(4), 399–405. https://doi.org/10.1016/j.jare.2017.05.005

Ye, X., Lu, F., Yao, T., Gan, R., & Sui, Z. (2016). Optimization of reaction conditions for improving nutritional properties in heat moisture treated maize starch. *International Journal of Biological Macromolecules*, *93*, 34–40. https://doi.org/10.1016/j.ijbiomac.2016.08.057

Zeng, F., Ma, F., Kong, F., Gao, Q., & Yu, S. (2015). Physicochemical properties and digestibility of hydrothermally treated waxy rice starch. *Food Chemistry*, *172*, 92–98. https://doi.org/10.1016/j.foodchem.2014.09.020